Journal of Thermal Analysis and Calorimetry, Vol. 74 (2003) 227–236

CURING KINETICS AND THERMAL PROPERTY CHARACTERIZATION OF BISPHENOL-F EPOXY RESIN AND MeTHPA SYSTEM

H. Zhao [2,1], *J. Gao* [1]*, *Y. Li* [1] *and S. Shen* [1]

[1]College of Chemistry and Environmental Science, Hebei University, Hebei, Baoding 071002,
P. R. China
[2]Department of Chemistry, Baoding Teachers College, Hebei, Baoding 071051, P. R. China

(Received October 31, 2002; in revised form February 4, 2003)

Abstract

The curing kinetics of bisphenol-F epoxy resin (BPFER) and curing agent 3-methyl-1,2,3,6-tetrahydrophthalic anhydride (MeTHPA), with N,N-dimethyl-benzylamine as an accelerator, were studied by differential scanning calorimetry (DSC). Analysis of DSC data indicated that an autocatalytic behavior showed in the first stages of the cure for the system, which could be well described by the model proposed by Kamal, which includes two rate constants, k_1 and k_2, and two reaction orders, m and n. The curing reaction at the later stages was practically diffusion-controlled. To consider the diffusion effect more precisely, diffusion factor, $d(\alpha)$, was introduced into Kamal's equation. The glass transition temperatures (T_gs) of the BPFER/MeTHPA samples were determined by means of torsional braid analysis (TBA). The thermal degradation kinetics of cured BPFER were investigated by thermogravimetric analysis (TG).

Keywords: bisphenol-F epoxy resin, glass transition temperature, kinetics,
3-methyl-1,2,3,6-tetrahydrophthalic anhydride, thermal degradation

Introduction

Bisphenol-A epoxy resin (BPAER) is widely used in the polymer industry for coatings, adhesives, insulating materials and polymer matrices for composite materials, *et al.* Compared with BPAER, bisphenol-F epoxy resin has a lower viscosity and good processibility. It could well be applied in the liquid state at lower viscosity, [1,2], because it is not necessary to add reactive diluent or solvent into BPFER reaction system, and the thermal stability, chemical resistance and corrosion resistance especially do not decrease.

Studies of BPFER's applications [3, 4] and physical properties [5] have been reported on extensively in recent years. However, descriptions of cure kinetics of the BPFER/MeTHPA system have been lacking until now. In order to provide a basis for curing process theory for the applications of BPFER, it is necessary to conduct research on the curing kinetics of the BPFER/MeTHPA system. Kamal's model [6], arising from an autocatalytic reaction mechanism, only described the first stage of cure due to the

---

* Author for correspondence: E-mail: gaojg@mail.hbu.edu.cn

1388–6150/2003/ $ 20.00
© 2003 Akadémiai Kiadó, Budapest

Akadémiai Kiadó, Budapest
Kluwer Academic Publishers, Dordrecht

gelation and vitrification. In the present article, therefore, the curing kinetics of MeTHPA-cured BPFER was evaluated by isothermal DSC. The Kamal kinetic model was also applied to isothermal DSC data. To take into account the diffusion effect, the Kamal model was extended by introduction of a diffusion factor, $d(\alpha)$. The glass transition temperature and the thermal degradation kinetics were investigated by torsional braid analysis (TBA) and thermogravimetric analysis (TG), respectively. The relationship between T_gs and the molar ratio of carboxyl group to epoxy group was discussed. TG data was analyzed according to literature [7, 8]. Structure changes during the curing process were investigated by Fourier transformation infrared spectroscopy (FTIR).

Experimental

Materials

Bisphenol-F was recrystallized from toluene, and a crystal with a melting point of 435 K was obtained. Epichlorohydrin, NaOH, KOH, acetone, ethylalcohol, hydrochloric acid, N,N-dimethylbenzylamine and curing agent 3-methyl-1,2,3,6-tetrahydrophthalic anhydride were all analytically pure grade and were supplied by Beijing Chemical Reagent Co.

Synthesis of BPFER

Epoxy resin based on bisphenol-F used in this work was synthesized according to Rainer *et al*. [9]. The molecular structure of this resin has the following approximate form.

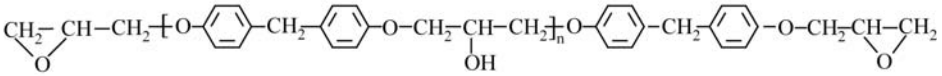

where n=0, 1. The epoxy value was determined according to Jay [10] to be 0.507 mol 100 g^{-1}.

IR measurements

The BPFER/MeTHPA samples were prepared with a stoichiometric ratio of one epoxy group with one carboxyl group. During the isothermal curing, an FTS-40 IR spectrophotometer (FTIR, BIO-RAD Co., USA) was used for the investigation of the structure changes of the curing system [11]. The sample was dissolved in chloroform, then was coated into a thin film on a potassium bromide plate. Chloroform was completely evaporated in vacuum. We named the uncured sample as sample A. Sample A was scanned by FTIR, then was placed in a heated oven at a fixed temperature at 373 K for 120 min (sample B). Sample B was scanned by FTIR, then was cured successively at 423 K for 120 min (sample C). Sample C was analyzed by FTIR.

DSC method

Curing studies were carried out by a Shimadzu DT-41 differential scanning calorimeter (Shimadzu Co., Japan). The DSC was calibrated with high-purity indium,

α-Al_2O_3 was used as the reference material. Isothermal and dynamic-heating experiments were carried out according to Opalicki *et al*. [12] under a nitrogen flow of 40 mL min^{-1}.

BPFER and curing agent MeTHPA with an accelerator N,N-dimethylbenzylamine were used as received and mixed homogeneously at a 1:1 molar ratio of carboxyl group to epoxy group. Samples of approximately 10 mg of the mixture were weighed accurately into an aluminum DSC sample pan and sealed with an aluminum lid. The entire operation was carried out in a dry chamber.

Samples were placed in the thermostatic baths at a curing temperatures T_c, 394, 401, 408 and 413 K, respectively. The reaction was considered complete when the rate curve leveled off to a baseline. The total area under the exothermal curve, based on the extrapolated baseline at the end of reaction, was used to calculate the isothermal heat of cure, ΔH_i, at a given temperature. After each isothermal run, the sample was quenched to 283 K and then reheated at 10 K min^{-1} to 573 K in order to determine the residual heat of reaction, ΔH_r. The total heat evolved during the curing reaction is $\Delta H_0 = \Delta H_i + \Delta H_r$.

Torsional braid analysis (TBA)

Specimens, prepared by dipping heat-cleaned glass fiber braid in the acetone solution of BPFER/MeTHPA system and an accelerator mixed homogeneously at different molar ratio. The molar ratio of carboxyl group to epoxy group was 0.6:1, 0.8:1, 1:1, 1.1:1 and 1.2:1, and marked with No. 1, 2, 3, 4 and 5, respectively, then acetone was completely evaporated in vacuum. The air oven was first heated up to 373 K, and kept for a certain period of time until the system reached the equilibrium state. Specimens were quickly set into the thermostatic baths for 120 min. Then the air oven was reheated up to the temperature of 423 K. Specimens were kept in the thermostatic baths for 600 min, then taken out and cooled to room temperature, and their T_gs were determined using torsional braid analysis [12, 13] with the heating rate of 2 K min^{-1}.

TG measurement

Samples of BPFER/MeTHPA of No. 1, 2, 3, 4 and 5 were cured at 373 K for 120 min and at 423 K for 600 min, respectively. Thermal analysis was carried out on a Shimadzu DT-40 thermogravimetric analyzer (TG) under a nitrogen flow of 40 mL min^{-1}. About 4 mg of the sample, which had been completely cured, was put into a platinum cell and placed on detector places, then the furnace was heated to 923 K at a heating rate of 10 K min^{-1}.

Results and discussion

Isothermal curing

The FTIR spectrums of BPFER/MeTHPA system detected are shown in Fig. 1. The most significant feature is the appearance of the epoxide group absorption at 914 cm^{-1} (marked

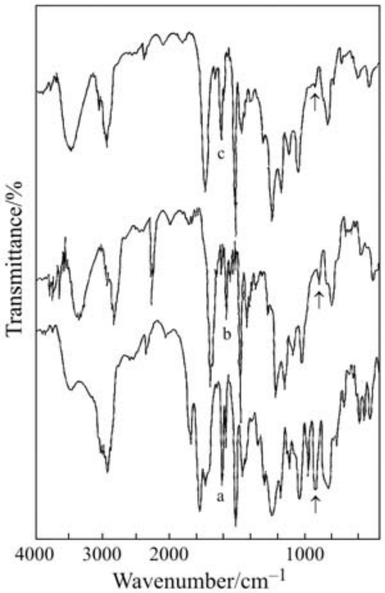

Fig. 1 FTIR spectrum of BPFER/MeTHPA after curing for a – non-cured BPFER; b – BPFER cured at 373 K for 120 min; c – BPFER cured at 373 K for 120 min and 423 K for 120 min

by an arrow). It is observed that this absorption peak of BPFER/MeTHPA cured at 373 K for 120 min (sample B) becomes much lower than that of non-cured BPFER (sample A), and the absorption peak of sample C becomes a tiny peak. The absorbance (914 cm^{-1}) of each sample was shown in Table 1. We can see that the absorbance decreased with the curing time increasing.

Table 1 Absorbance of BPFER/MeTHPA for different samples

Sample	Absorbance
A	0.391
B	0.074
C	0.039

The mechanisms of the curing reaction of thermosetting resins have the two general kinetic models; that is, n^{th}-order and an autocatalytic one [7]. The reaction rate of n^{th}-order kinetics can be expressed as:

$$\frac{\mathrm{d}\alpha}{\mathrm{d}t} = k(T)\,(1-\alpha)^{\mathrm{n}} \tag{1}$$

$k(T)$ is the specific rate constant, which is function of the temperature. The reaction rate of autocatalytic kinetics can be defined as:

$$\frac{d\alpha}{dt} = k'\alpha^{m}(1-\alpha)^{n} \tag{2}$$

where α is the extent of reaction, and α is given by $\alpha=\Delta H_t/\Delta H_0$, where ΔH_t is the partial area under a DSC trace up to time t; m and n are the reaction orders and k' is the kinetic rate constant.

To take into account the autocatalytic reaction, where initial reaction rate of an autocatalytic reaction is not zero, Kamal [6] proposed the generalized expression:

$$\frac{d\alpha}{dt} = (k_1 + k_2\alpha^{m})(1-\alpha)^{n} \tag{3}$$

where k_1 and k_2 are the specific rate constants, which are functions of the temperature.

According to n^{th}-order kinetic model, the maximum reaction rate will be observed at t=0, while according to the autocatalytic model, the reaction rate is zero initially and attains the maximum value at some intermediate conversion.

During the curing reaction of the thermosetting resins, the heat of reaction released at any time is proportional to the number of moles reacted at that time, namely, the released heat is proportional to the extent of the reaction [17, 18]. If the cure reaction is the only thermal event, then the reaction rate $d\alpha/dt$ is proportion to the heat flow [7], dH/dt, that is:

$$\frac{d\alpha}{dt} = \frac{dH/dt}{\Delta H_0} \tag{4}$$

So, the curing kinetics were studied and the kinetics data were determined [19, 20].

Figure 2 shows plots of the curing reaction conversion α *vs.* time t at different isothermal temperatures, and isothermal DSC curves are shown in Fig. 3 plotted as $d\alpha/dt$ *vs*. time t. The reaction rate at any temperature increases with time at the initial stage of cure and passes through a maximum. The peak of reaction rate becomes higher and shifts to shorter time with an increase in isothermal temperature. The plots show a maximum reaction rate at time $t>0$, thereby negating simple n^{th}-order kinetics. To compute kinetic parameters in Eq. (3), several methods have been proposed [21–23]. In this study, k_1 was graphically calculated as the initial reaction rate at time t=0, given by the intercept of Fig. 3. Then, k_2, m and n were calculated through non-linear regression according to Eq. (3). The resulting data obtained from this method for all isothermal experiments are shown in Table 2.

Table 2 Kinetic parameters for isothermal curing of BPFER/MeTHPA

Parameter	T/K			
	394	401	408	413
k_1 ($\cdot 10^{-4}$ s^{-1})	8.76	10.30	11.20	13.10
k_2 ($\cdot 10^{-3}$ s^{-1})	2.89	4.13	7.84	10.30
m	0.74	0.77	0.83	0.64
n	1.39	1.46	2.01	1.45

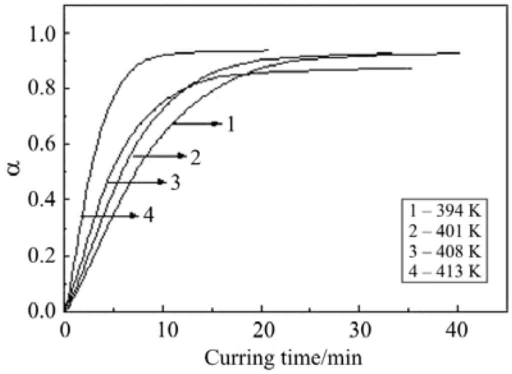

Fig. 2 Conversion, α, *vs*. time *t* curves at different curing temperatures

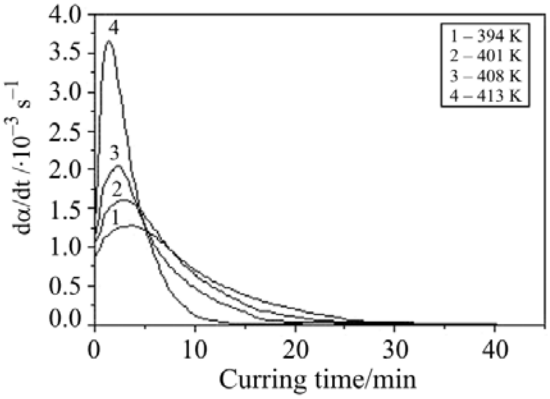

Fig. 3 Reaction rate, dα/d*t*, *vs*. time *t* curves at different curing temperatures

As seen from Table 2, k_1 values are small compared with those obtained for k_2, which affect the reaction more. Furthermore, k_1 and k_2 values increase with the curing temperature.

Typical comparisons between the experimental DSC data and the autocatalytic model with Eq. (3) determined parameters are shown in Fig. 4. At early stages of cure, before gelation and vitrification, the reaction takes place in the liquid phase and is controlled by chemical kinetics. So, the kinetic behavior described by this model coincides with the experimental data. As the reaction progresses, a deviation appears due to the onset of gelation and vitrification where the mobility of reactive groups is hindered, and the rate of conversion is controlled by diffusion rather than by kinetic factors [24]. Differences between model predictions and experimental data were observed. This can be interpreted by free volume consideration [25]: the free volume of materials decreased with curing reaction conversion increasing, then the rate of diffusion of reactive groups reduced, leading to decreasing reaction rate.

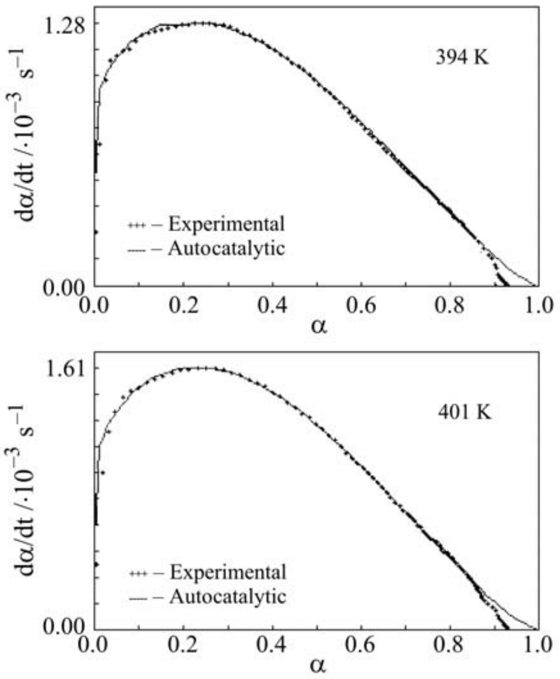

Fig. 4 Comparisons of experimental data with theoretical values calculated from Eq. (3). Reaction rate dα/dt, *vs*. conversion α at 394 and 401 K

To consider the diffusion effect more precisely, a semiempirical relationship, based on the free volume consideration, was proposed by Chern and Poehlein [25]. In this relationship, ‘diffusion factor’, $d(\alpha)$, was defined with two empirical parameters as follows:

$$d(\alpha)=\frac{1}{1+\exp[C(\alpha-\alpha_c)]} \tag{5}$$

where C is the diffusion coefficient and α_c is the critical conversion depending on the curing temperatures. The plots of $d(\alpha)$ *vs*. conversion α at different curing temperatures are shown in Fig. 5. For $\alpha \ll \alpha_c$, $d(\alpha)$ approximately equals unity and the effect

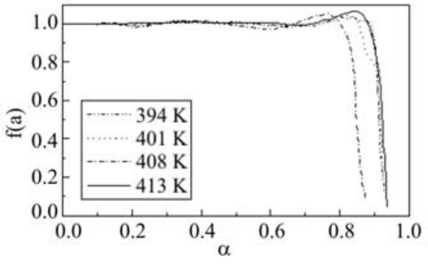

Fig. 5 Plot of diffusion factor $d(\alpha)$ *vs*. conversion α at different curing temperatures

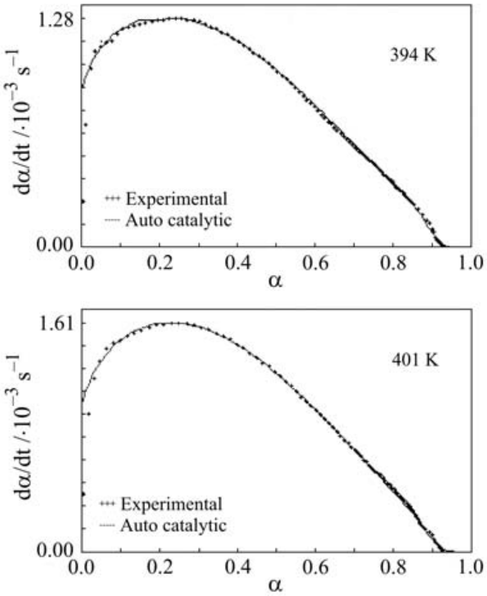

Fig. 6 Comparisons of experimental data with theoretical values calculated from Eq. (6). Reaction rate dα/dt, *vs*. conversion α at 394 and 401 K

of diffusion is negligible, so that the reaction is kinetically controlled. As α approaches α_c, $d(\alpha)$ begins to decrease, reaching a value of 0.5 at $\alpha=\alpha_c$. Beyond that point, it continues to decrease and approaches zero, which means that the reaction becomes very slow and effectively stops.

Considering the diffusion effect, the reaction rate of cure can be expressed in the following form to account for the effects of diffusion.

$$\frac{\mathrm{d}\alpha}{\mathrm{d}t}=(k_1+k_2\alpha^{\mathrm{m}})(1-\alpha)^{\mathrm{n}}\frac{1}{1+\exp[C(\alpha-\alpha_{\mathrm{c}}]} \tag{6}$$

Figure 6 shows the comparison between experimental values and those obtained from Eq. (6). The calculated values agree very well with experimental data. Thus we employ the proposed generalized kinetic model to predict and describe the advance of this epoxy resin system as a function of the curing temperature.

Measurement of T_g value

T_g has been used directly as a parameter for conversion in analysis of reaction kinetic models [26, 27], and there is a one-to-one relationship between the T_g and the degree of cure. It is a convenient parameter because of the ease of measurement of T_g by TBA, and it is particularly useful at high conversion and after vitrification because of the nonlinearity of T_g *vs*. conversion reaction [28, 29]. T_gs *vs*. the molar ratio of carboxyl group to epoxy group are shown in Table 3. As seen from Table 3, the T_g attain the maximum value when the molar ratio of carboxyl group to epoxy group was 0.8:1.

Table 3 Values of T_g, T_0, $T_{1/2}$, E_1 and E_2 of completely cured BPFER

Parameter	Molar ratio of carboxyl group to epoxy group				
	0.6:1	0.8:1	1:1	1.1:1	1.2:1
T_g/K	336.2	338.0	335.0	332.1	334.5
T_0/K	545	563	519	513	496
$T_{1/2}$/K	727	711	690	688	686
E_1/kJ mol^{-1}	23.02	27.71	–	–	–
E_2/kJ mol^{-1}	290.03	157.03	–	–	–

Thermal degradation

The TG trace of MeTHPA-cured BPFER revealed two degradation steps under a nitrogen flow of 40 mL min^{-1}. The following kinetic equation was assumed to hold for the thermal degradation reaction [7, 8].

$$\ln\left(\frac{C}{T^{1.92}}\right)=\ln\frac{AE}{\phi R}+3.77-1.92\ln E-\frac{E}{RT} \tag{7}$$

where $C=W/W_0$, W is the remaining mass, W_0 is the total mass, E is the degradation activation energy, A is the frequency factor, ϕ is the heating rate, and R is the ideal gas constant.

The degradation activation energy of different samples can be calculated from the plots of $\ln(C/T^{1.92})$ *vs*. $1/T$. E_1 and E_2 were the degradation activation energy of the first and the second stage, and the values were shown in Table 3. T_0 and $T_{1/2}$ are the temperatures at which the mass loss are 0 and 50 percent, respectively. As seen from Table 3, the degradation activation energy in the second stage is much higher than that in the first stage, illustrating that the breaking of strong bonds takes place in the second stage, while weak bonds were broken in the first stage. T_0 increases with the increment of the molar ratio of carboxyl group to epoxy group. When the molar ratio is 0.8:1, T_0 attains the maximum value, then the value decreases. $T_{1/2}$ decreases with the molar ratio of carboxyl group to epoxy group increasing.

From Table 3, we can draw a conclusion that the optimum molar ratio of carboxyl group to epoxy group is 0.8:1. Because at this point, T_g and T_0 have the maximum values. When the molar ratio of carboxyl group to epoxy group is low at 0.6:1, the T_g and T_0 become lower, but $T_{1/2}$ is higher. The T_gs, T_0s and $T_{1/2}$s are all lower at another three molar ratios. The reason is that part of carboxyl group doesn't react with BPFER during curing when the proportion of carboxyl group increases.

Conclusions

The cure reaction for the system of BPFER/MeTHPA system is shown to be autocatalytic kinetic behavior in the first stage, which can well be described with the model proposed by Kamal [6]. The curing reaction at the later stage was practically diffusion-controlled. To consider the diffusion effect more precisely, $d(\alpha)$, was introduced into Kamal's equation which is possible to describe and predict the cure reaction of this epoxy resin (Eq. 6). The theoretical values agree very well with the experimental data.

- T_gs were investigated for BPFER/MeTHPA samples cured completely at different molar ratio of carboxyl group to epoxy group. The results show that the T_g attain the maximum value when the molar ratio of carboxyl group to epoxy group was 0.8:1.
- TG trace of this system revealed two decomposition stages. E_2 is much higher than E_1. When the molar ratio is 0.8:1, T_0 has the maximum value. $T_{1/2}$ decreases with the increment of the molar ratio of carboxyl group to epoxy group. To take effects of T_g, T_0 and $T_{1/2}$ into account, the optimum molar ratio of carboxyl group to epoxy group is 0.8:1.

References

1 B. Louis, P. Bo, J. Sonva and M. Jan-Anders, Proc. Int. Conf. Compos. Mater., 6 (1995) 389.
2 H. Hideo and I. Akihiro, Jpn. Kokai Tokkyo Koho JP 11116662, 1999.
3 O. Toshiaki, Jpn. Kokai Tokkyo Koho JP 07292072, 1995.
4 W. Ivo, W. Ludmila, B. Vaclav, K. Ludek, M. Vladimer, M. Pravoslav and R. Antonin, Czech Rep. CZ 280402, 1996.
5 M. Kasen and R. Santoys, Cryogenics, 35 (1995) 731.
6 M. R. Kamal, Polym. Eng. Sci., 14 (1974) 231.
7 Z. Liu, Introduction of thermal analysis. Beijing: Chemical Industry Publishing Co. 1991, p. 100.
8 P. M. Madhusudanan, K. Krishnan and K. N. Ninan, Thermochim. Acta, 97 (1986) 189.
9 E. Rainer, G. Udo, H. W. Heinrich and B. Eruin, Ger. Pat., 1985, DD228, 279.
10 R. R. Jay, Anal. Chem., 36 (1964) 665.
11 S.-G. Hong and C.-S. Wu, J. Therm. Anal. Cal., 59 (2000) 711.
12 M. Opalicki, J. M. Kenny and L. Nicolais, J. Appl. Polym. Sci., 61 (1996) 1025.
13 J. K. Gillham, In Techniques and Methods of Polymer Evaluation Vol. 2, New York, Marcel Dekker 1970, p. 225.
14 R. F. Boyer, Polymer, 17 (1976) 996.
15 G. Liu, L. Zhang, X. Qu, Y. Li, J. Gao and L. Yang, J. Therm. Anal. Cal., 65 (2001) 837.
16 F. Yang, K. D. Yao and W. Koh, J. Appl. Polym. Sci., 73 (1999) 1501.
17 E. M. Woo and J. C. Seferis, J. Appl. Polym. Sci., 40 (1990) 1237.
18 M. Ghaemy and M. H. Riahy, Eur. Polym. J., 32 (1996) 1207.
19 M. R. Keenan, J. Appl. Polym. Sci., 33 (1987) 1725.
20 J. M. Barton, Adv. Polym. Sci., 72 (1985) 111.
21 M. E. Ryan and A. Dutta, Polymer, 20 (1979) 203.
22 A. Moroni, J. Mijiovic, E. M. Pearce and C. C. Foun, J. Appl. Polym. Sci., 32 (1986) 3761.
23 J. M. Kenny, J. Appl. Polym. Sci., 51 (1994) 761
24 K. C. Cole, J. J. Hechler and D. Noel, Macromolecules, 24 (1991) 3098.
25 C. S. Chern and G. W. Poehlein, Polym. Eng. Sci., 27 (1987) 788.
26 S. L. Simon and J. K. Gillham, J. Appl. Polym. Sci., 47 (1993) 461.
27 G. Wisanrakkit and J. K. Gillham, J. Appl. Polym. Sci., 41 (1990) 2885.
28 R. A. Venditti and J. K. Gillham, J. Appl. Polym. Sci., 64 (1997) 3.
29 G. Wisanrakkit, J. K. Gillham and J. B. Enns, J. Appl. Polym. Sci., 41 (1990) 1895.